Extended breakdown of Simpleman approximation

J. Tian*, X. Wang, and J. H. Eberly

Rochester Theory Center and the Department of Physics and Astronomy, University of Rochester, Rochester, New York 14627, USA

**Corresponding author: jtian@pas.rochester.edu*

Received October 24, 2012; accepted November 16, 2012; posted online December 28, 2012

In this letter, we solve three-dimensional time-dependent Newton equations for atoms interacting with a ten-cycle elliptically polarized laser pulse. The ionized electron momentum distributions show a tilt angle between the distribution density peak and the main polarization axis. The tilt angle's behavior changes with an increasing laser intensity. We show that this behavior change is directly related to the release time of the electron from the atom.

OCIS codes: 000.0000, 000.1600, 000.4430.
doi: 10.3788/COL201311.010001.

In the high-field regime of atomic and molecular physics, where near-optical laser intensities are in the range of $10^{14} - 10^{17}$ W/cm^2, the force on a bound electron from the laser field is comparable to the Coulomb forces from both the ionic core and any other electrons. Atomic and molecular electron reactions in this intensity range are being exploited for ongoing pioneering studies such as attosecond pulse generation[1], electron rescattering spectroscopy[2], and new observations of tunneling times[3]. The high field strength associated with these phenomena has eliminated ordinary radiative perturbation theory as a useful tool, and has led to the development of alternative theoretical approaches[4]. However, since many of the observed effects are determined largely by the behavior of electrons after or long after they have been released from their ion, the so-called Simpleman theoretical approach[5], which assumes that the field strength is high enough to ignore non-laser forces altogether, has been repeatedly and remarkably successfully used for interpretation of experimental data.

Recently, experiments have been able to examine outgoing electron dynamics sufficiently finely to begin to allow deviations from the Simpleman picture to be captured and analyzed. This has been done, for example, by using circular and elliptical polarization to promote off-axis electron trajectories[6,7], or by deliberately inspecting trajectories at right angles to a linear polarization axis[8]. The response of an electron to elliptically polarized light reveals effects not available under probing by linearly polarized light. For example, when the major (x) polarization axis is scanned, the ion momentum distribution has a single peak, but it has two peaks along the minor (y) axis. These features are both evident in Fig. 1, and have been observed repeatedly[9,10]. Both are well-explained[11] by the Simpleman theory, but the centers of the distributions clearly tilt away from vertical in the figure, and this is not a Simpleman feature. It has been explored recently as a function of laser intensity[7], and is interpreted as a consequence of residual Coulombic attraction from the ion as the electron departs.

Elliptical polarization studies at high field strengths have also been carried out in double ionization[10–15], where again the finite ellipticity provides access to effects not as easily visible with linear or circular polarization, such as delayed release times of the two electrons[16,17]. These have also been successfully analyzed theoretically[18–19], although interesting questions remain open[20].

In the experiments of immediate interest[7], elliptically polarized laser pulses were used to generate singly ionized helium and argon ions. According to the experimental results shown in Fig. 2, the tilt angle is a function of intensity. One sees that the tilt angles of He are approximately independent of increasing laser intensity, and the tilt angles of Ar are almost constant, showing a slight decreasing trend. We will label this as 'plateau' behavior as a function of intensity. A typical tunneling model[21–23] has been applied in Ref. [7], but fails to explain the slight differences between Ar and He. However, a new semi-classical model was used to examine the descrepancy, introducing the argument that atomic polarizability should be considered as a significant influence in the tunneling process[24].

Our interest here is in understanding the intensity-dependences of the tilt angle, as shown in Fig. 2, and more particularly in extending tilt-angle study to higher intensities. We do this by calculating electron trajectories from beginning to end of the laser pulse for a statistical ensemble of one million atoms, from which numerical x-y momentum distributions as in Fig. 3 are

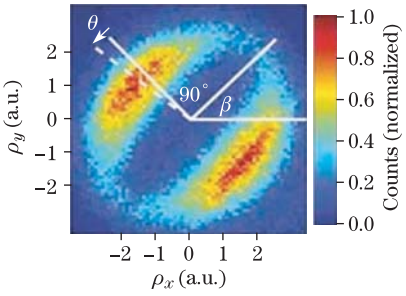

Fig. 1. Ion momentum distribution following ionization of He by an elliptically polarized with 7-fs pulse duration Ti:sapphire laser pulse (λ-740 mm) and ellipticity 0.78. Here θ is the interesting angle of tilt away from the main (x) polarization axis[7].

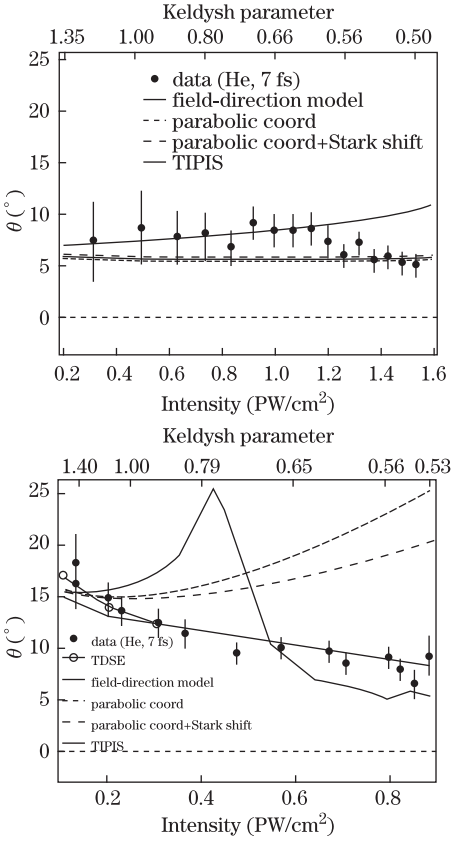

Fig. 2. Experimental results for He and Ar, as reported in Ref. [7] showing changes in tilt angle over a range of relatively low intensities, along with a group of theoretical mode1 predictions.

obtained. This model of ionization takes account of the entire ionization process and all active forces both before and after electron release. Then intensity-dependent trends as in Fig. 2 can be constructed and compared with existing data.

Our electron trajectories are obtained by the familiar method[25−27] of *ab initio* numerical solution of the appropriate time-dependent Newton equations (TDNE). Naturally, one would prefer a more sophisticated approach, but it is commonly understood[4] why *ab initio* high-field solutions of the time-dependent Schrödinger equation (TDSE) are beyond current computational capability for arbitrary laser polarization. One exception is He[28] under linear laser polarization. For our TDNE solutions, we have used a known one-electron atom model[29,30] in which a ground-state bound electron is exposed to the existing forces from the laser field and the ion beginning at laser turn-on. Different atomic species are distinguished by their different values of ionization potential. The Hamiltonian of our electron in an elliptically polarized laser field can be expressed as follows in atomic units (a.u.):

$$H = -\frac{1}{\sqrt{a^2+r^2}} + \frac{p^2}{2} + \vec{F}(t)\cdot\vec{r}, \qquad (1)$$

$$\vec{F}(t) = E_0 f(t)[\hat{x}\cos(\omega t+\phi) + \hat{y}\varepsilon\sin(\omega t+\phi)], \qquad (2)$$

with a sine-squared pulse envelope: $f(t) = \sin^2(\pi t/T)$.

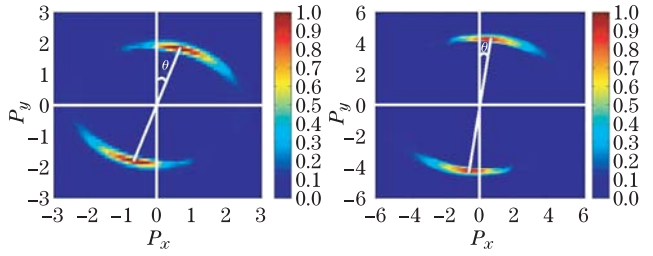

Fig. 3. Two examples of electrons' momentum distribution, Electrons are ionized by a 10-cycle pulse. Upper panel: He with intensity I=6.6 PW/cm^2; Lower panel: Ar with intensity I=2.2 PW/cm^2.

Here, the first term of the Hamiltonian provides the model's ion-electron attraction, r is the radius from the ion to the electron, and a is a parameter that adjusts the atom model's ionization potential. For He we have $a = 1.0$ and for Ar $a = 1.5$. The second term is the kinetic energy and the third term is the electron-field interaction. Since we assume that the laser field is propagating in the z direction, the field vector $\vec{F}(t)$ rotates in the x-y plane, with $f(t)$ as the pulse envelope function, and T is the total pulse duration. In the simulations, we used an anti-clockwise rotation for the field. The phase angle ϕ is assigned random values from 0 to 2π. We used a 10-cycle pulse with ellipticity $\varepsilon = 0.8$. The results for our TDNE momentum distributions, as shown in Fig. 3, display tilt angles similar to those found experimentally, as shown in Fig. 1.

We can divide the x and y momenta into contributions from the Coulomb force and the force of the laser field: $\vec{p} = \vec{p}_{\rm C} + \vec{p}_{\rm E}$. The Coulomb force is quite small, and has negligible effect on p_y, as is evident from the small tilt angles observed, so a good approximation for θ can be written as

$$\theta \approx \tan\theta = \frac{p_x}{p_y} = \frac{p_{x\rm C}+p_{x\rm E}}{p_{y\rm C}+p_{y\rm E}} \approx \frac{p_{x\rm C}+p_{x\rm E}}{p_{y\rm E}}. \qquad (3)$$

Thus, from the momentum peaks such as in Fig. 3, tilt angles can be determined and plotted as a function of intensity, and the TDNE results produce the lines in Fig. 4. Note that Fig. 4 goes to intensities significantly beyond those included in Fig. 2, toward and slightly beyond the saturation intensities of the He and Ar atoms. At these higher intensities new behavior is evident, with clear changes to the relatively flat 'plateau' behavior shown at the low-intensity side, where there is rough agreement with Fig. 2. These departures from plateau-type behavior are given attention in the following paragraphs.

The striking element in our extended-intensity tilt-angle results shown in Fig. 4 is the semi-regularity of relatively abrupt drops in value as the intensity increases. We believe that these can be interpreted as arising from a dependence on t_0, the release time of the electron from its ion, as follows.

We first note that the most probable release time obviously occurs at the time of peak intensity $I_{\rm pk}$. This time is fixed at the peak of the field envelope, and remains the same no matter what the peak intensity is, given the same number of cycles in the pulse. So the tilt angle, according to this reasoning, should be independent

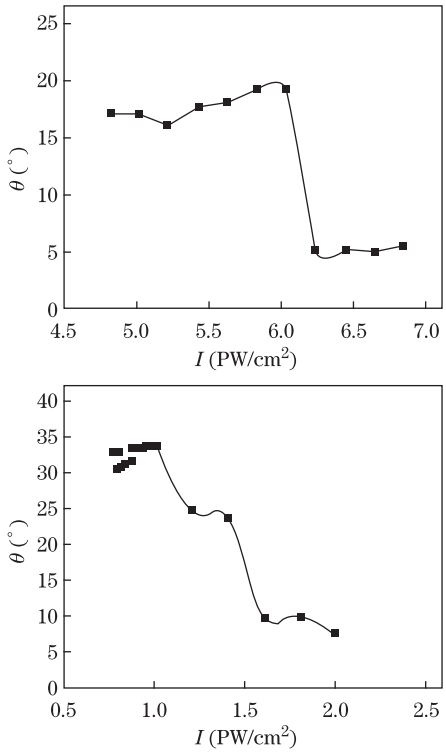

Fig. 4. Tilt angles versus higher intensity obtained by TDNE calculations for a 10-cycle elliptically polarized pulse. Upper panel: He, and lower panel: Ar. The solid lines smoothly connect data points obtained from momentum distributions such as shown in Fig. 3, calculated for intensity values from 4.8 to 6.8 PW/cm^2 for He and from 1.0 to 2.0 PW/cm^2 for Ar in intervals of 0.2 PW/cm^2. The Ar curve shows a left-hand addition from 0.76 to 1.0 PW/cm^2 with an interval of only 0.02 PW/cm^2, in order to compare with the flat end of the narrow range of experimental data for Ar in Fig. 2.

of intensity. We believe this is the main reason for the plateau behavior of tilt angle on intensity shown in the experimental data in Fig. 2, as well as in the lefthand ends of our results in Fig. 4.

This reasoning fails, however, to account for the extended intensities in the figure, near and particularly above saturation intensity I_s. As soon as the peak intensity is increased above the saturation intensity, the electron experiences the saturation value earlier in the pulse, and then the electron release occurs earlier. Earlier electron release and higher laser intensity work together to ensure that the electron is free for a longer portion of the pulse and in a stronger field, i.e., it experiences conditions where the Simpleman approximation is more nearly accurate. This is exactly right for a smaller tilt angle.

Such an intuitive analysis can be made semi-quantitative with reference to Fig. 5. Since the x-axis is the major axis, the rate of ionization is greatest at maxima of F_x. For a laser pulse with peak intensity I_{pk} below the saturation level I_s, the time t_0 is always found around $I \approx I_{pk}$, shown as point 1 in Fig. 5. However, as higher intensities are utilized, the magnitude of the next earlier field oscillation peak (shown as point 2 in Fig. 5) may reach the saturation line. This means that t_0 takes an earlier value. The amount of accumulated momentum is obviously dependent on the time available for exposure

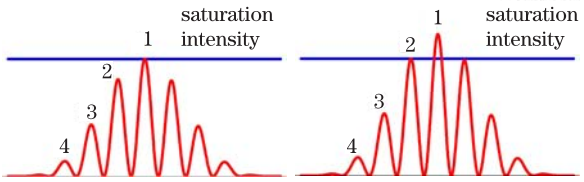

Fig. 5. (Color online) Horizontal line is the saturation line. The red line is the x component of the laser intensity. Left panel: I_{pk}=I_s. Right panel: I_{pk}>I_s.

to the existing forces. Thus if there is a shift of t_0 to an earlier value, we should expect a decrease of the tilt angle value. That effect is evident for He in Fig. 4.

Going further, on the basis of this argument one may expect that multiple shifts of t_0 can occur for atoms that have lower I_s values as intensity is increased, since the saturation intensity can be reeached at more than one pre-peak field cycle. It appears that we see this phenomenon in Ar in Fig. 4. According to that figure, the shift happens twice - t_0 changes from 1 to 2, then from 2 to 3 for Ar. In the figure there is only one downward shift in the He plot.

In conclusion, we have made classical TDNE calculations of electron ionization trajectories under elliptically polarized high-field pulses. These provided ion momentum distributions (recall Fig. 1) yielding the typical double peak along the minor axis, but also a small displacement along the major axis, an effect not compatible with the Simpleman approximation[5], but in qualitative agreement with experimental results and previous calculations. We have extended the examination of this non-Simpleman effect by increasing the range of intensities under examination. The extension to greater intensities reveals additional structural features in the dependence of the tilt angle on intensity.

From the TDNE results, we speculatively conclude that for low intensities the tilt angle should show little or no dependence on intensity, and should be generically the same for all atoms. This is basically the behavior exhibited in the experimental results for Ar and He: before the intensity reaches the saturation point, the tilt angles remain roughly constant. When the intensity reaches the saturation point, the tilt angles start to decrease, and do so in a roughly regular way. This is because the tilt angle is stongly connected to the value of t_0, the time point of highest ionization rate. This time point always happens around a peak of the field oscillation.

In cases where the laser peak intensity is below the saturation intensity, ionization occurs at the intensity peak. However, if the laser peak intensity is higher than the saturation intensity, a field peak sufficient to ionize will occur sooner than the intensity peak. Thus, as a function of increasing peak intensity, earlier and earlier times will serve as the effective ionization time. Between shifts from one t_0 value to the next earlier one a plateau in tilt angle will occur. The TDNE trajectory calculations replicate the experimental tendency for tilt angles to vary only little over a range of relatively low intensities, below and well below saturation. However, when extended to higher intensities in and above the saturation intensity, these new features are found.

This work was supported by the DOE under Grant No.

DE-FG02-05ER15713.

References

1. M. Ivanov and F. Krausz, Rev. Mod. Phys. **81,** 163 (2009).
2. P. B. Corkum, Phys. Today **64,** 36 (2011).
3. P. Eckle, A. N. Pfeiffer, C. Cirelli, A. Staudte, R. Dorner, H. G. Muller, M. Buttiker, and U. Keller, Science **322,** 1525 (2008).
4. W. Becker, X. J. Liu, P. J. Ho, and J. H. Eberly, Rev. Mod. Phys. **84,** 1011 (2012).
5. H. B. V. Linden, V. D. Heuvell, and H. G. Muller, in *Multiphoton Processes*, edited by S. J. Smith and P. L. Knight (Cambridge University Press, 1988) p. 31.
6. W. Chu, M. Wu, B. Zeng, J. Yao, H. Xiong, H. Xu, Z. Lin, and H. Kang, Phys. Rev. A **85,** 021403 (2012).
7. A. N. Pfeiffer, C. Cirelli, M. Smolarski, D. Dimitrovsky, M. Abu-samha, L. B. Madsen, and U. Keller, Nature Phys. **8,** 76 (2012).
8. P. A. Korneev, S. V. Popruzhenko, S. P. Goreslavski, T. M. Yan, D. Bauer, W. Becker, M. Kubel, M. F. Kling, C. Rodel, M. Wunsche, and G. G. Paulus, Phys. Rev. Lett. **108,** 223601 (2012).
9. C. M. Maharjan, A. S. Alnaser, X. M. Tong, B. Ulrich, P. Ranitovic, S. Ghimire, Z. Chang, I. V. Litvinyuk, and C. L. Cocke, Phys. Rev. A **72,** 041403 (R) (2005).
10. A. N. Pfeiffer, C. Cirelli, M. Smolarski, X. Wang, J. H. Eberly, R. Dörner, and U. Keller, New J. Phys. **13,** 093008 (2011).
11. X. Wang and J. H. Eberly, Phys. Rev. A **86,** 013421 (2012).
12. N. I. Shvetsov-Shilovski, S. P. Goreslavski, S. V. Popruzhenko, and W. Becker, Phys. Rev. A **77,** 063405 (2008).
13. X. Wang and J. H. Eberly, Phys. Rev. Lett. **103,** 103007 (2009).
14. X. Wang and J. H. Eberly, Phys. Rev. Lett. **105,** 083001 (2010).
15. X. Wang and J. H. Eberly, New J. Phys. **12,** 093047 (2010).
16. A. N. Pfeiffer, C. Cirelli, M. Smolarski, R. Dörner, and U. Keller, Nature Phys. **7,** 428 (2011).
17. K. Ueda and K. Ishikawa, Nature Phys. **7,** 371 (2011).
18. Y. Zhou, C. Huang, Q. Liao, and P. Lu, Phys. Rev. Lett. **109,** 053004 (2012).
19. X. Wang and J. H. Eberly, J. Chem. Phys. **137,** 22A542 (2012).
20. X. Wang, J. Tian, A. N. Pfeiffer, C. Cirelli, U. Keller, and J. H. Eberly, arXiv:1208.1516 (2012).
21. A. M. Perelomov, V. S. Popov, and M. V. Terent'ev, Sov. Phys. JETP **23,** 924 (1966).
22. M. V. Ammosov, N. B. Delone, and V. P. Krainov, Sov. Phys. JETP **64,** 1191 (1986).
23. X. M. Tong and C. D. Lin, J. Phys. B **38,** 2593 (2005).
24. N. I. Shvetsov-Shilovski, D. Dimitrovski, and L. B. Madsen, Phys. Rev. A **85,** 023428 (2012).
25. J. Javanainen, J. H. Eberly, and Q. C. Su, Phys. Rev. A **38,** 3430 (1988).
26. Q. C. Su and J. H. Eberly, Phys. Rev. A **44,** 5597 (1991).
27. S. L. Haan, Phys. Rev. Lett. **95,** 103008 (2006).
28. K. T. Taylor, J. S. Parker, D. Dundas, E. Smyth, and S. Vivirito, Laser Phys. **9,** 98 (1999).
29. J. Javanainen, J. H. Eberly, and Q. C. Su, Phys. Rev. A **38,** 3430 (1988).
30. Q. C. Su and J. H. Eberly, Phys. Rev. A **44,** 5597 (1991).